Water Chemistry

DOI: 10.1002/ange.200504159

Magic and Antimagic Protonated Water Clusters: Exotic Structures with Unusual Dynamic Effects**

*N. Jiten Singh, Mina Park, Seung Kyu Min, Seung Bum Suh, and Kwang S. Kim**

Protonated water species are key elements in dissociation and transport phenomena in aqueous chemistry and biological

[*] N. J. Singh, M. Park, S. K. Min, Dr. S. B. Suh, Prof. K. S. Kim
National Creative Research Initiative Center for Superfunctional Materials
Department of Chemistry
Division of Molecular and Life Sciences
Pohang University of Science and Technology
Pohang 790-784 (Korea)
Fax: (+82) 54-279-8137
E-mail: kim@postech.ac.kr

[**] This work was supported by CRI(KOSEF) and BK21. Most calculations were performed on supercomputers at KISTI.

Supporting information for this article is available on the WWW under http://www.angewandte.org or from the author.

systems. The investigation of protonated clusters $[H(H_2O)_n]^+$ is essential to understand the nature of protons in nanosized water droplets.[1–8] It has been known for a long time that in mass spectra, magic clusters ($n=21$) appear abundantly and antimagic clusters ($n=22$) appear scarcely or transiently.[4–7] For these clusters, diverse structures have been predicted.[8,9] The magic cluster has been suggested to have an aesthetic geometrical structure, a pentagonal dodecahedron (PD; 5^{12}),[4,5,7,9a] as related to water clathrates that trap methane and other gases in PD water cages.[10] In contrast, no convincing structure has been suggested for the antimagic cluster. Despite recent remarkable experimental progress,[4,5] no model has been successful in explaining the structures of both magic and antimagic clusters. There are few consistencies among experimental and theoretical models, and different empirical potentials predict different structures for these clusters. Therefore, accurate calculations of the magic/antimagic clusters have been called upon to correctly understand many existing experimental data.[11]

Our most accurate results give the answer to the following unresolved controversial issues: 1) why the magic and antimagic clusters exist; 2) whether the proton is inside or on the surface of the cage; 3) whether the proton is strongly bound to a single water molecule (Eigen form; H_3O^+) or is shared between two water molecules (Zundel form; $H_2O\cdots H^+\cdots OH_2$); 4) why a proton moiety is not observed in the IR spectra contrary to the theoretical prediction; 5) whether each spectrum corresponds to a particularly stable structure or many isomers; 6) why the OH stretching peak for AD-type H_d (in which A and D denote proton acceptor and donor, respectively, and H_d denotes a dangling hydrogen atom) is absent for the magic clusters and not appreciably measurable for the antimagic clusters at low temperatures,[5] which is in contrast to the strong AD peaks observed for other clusters; 7) any unknown thermal and dynamic effects of these clusters.

To search for experimentally relevant structures, we considered a number of energetically low-lying structures from those previously reported based on empirical potentials (though not consistent with ab initio results)[8,9] and many topologically different structures generated from our experience with various types of water-containing clusters.[12] Starting with these structures, we generated as many of the refined low-lying structures as possible at the level of the density-functional-based tight-binding theory (DFTB)[13] by using the simulated annealing/cooling method.[14] A more sophisticated basin-hopping method[9] was also employed, which gave consistent results with the above-mentioned method.

Since DFTB results (let alone existing empirical potential results) are not reliable, we refined the energies of the selected low-energy conformers by using Becke-3-Lee-Yang-Parr (B3LYP) calculations with the 6-31+G* basis set followed by the aug-cc-pVDZ$^+$ basis set (in which "+" denotes that the diffuse basis function of the hydrogen atom was removed). Again, Møller–Plesset second-order perturbation (MP2) calculations were performed for more-accurate energies.[15] The lowest-energy and nearly isoenergetic conformers identified with MP2 have been used for Car–Parrinello molecular dynamics (CPMD) simulations. Our experience with hydrogen-bonded clusters indicates that MP2 results are much more consistent with experiments than results obtained with density functional theory (DFT), which occasionally fails to predict realistic structures of water-containing clusters owing to its inability to include dispersion energy.[12] Indeed, for hydrogen-bonded systems, we observe that MP2 results are much more consistent with high-level ab initio calculations such as coupled-cluster theory. In this work, we also note that DFT fails to predict realistic structures, while MP2 explains the experimental data. More concrete results would be obtained at higher levels of ab initio theory.

In the case of the magic cluster of $[NH_4(H_2O)_{20}]^+$,[16] the NH_4^+ ion has four well-balanced, tetrahedrally oriented hydrogen bonds inside the cage and four unbalanced, strained hydrogen bonds on the surface. Thus, we find from our calculations that the cluster with the NH_4^+ ion inside the cage is more stable than the cluster with the NH_4^+ ion on the surface of the cage by about 2 kcal mol^{-1}. Similarly, we find that the magic clusters $[K(H_2O)_{20}]^+$ and $[Cs(H_2O)_{20}]^+$,[16] in which these alkali-metal cations have a coordination number greater than 4, also have internal structures because those cations can be tri- or tetra-coordinated (with strains) on the surface. In contrast, each hydrogen atom of the H_3O^+ ion involves a hydrogen bond as a strong hydrophilic site, whereas the oxygen atom of the H_3O^+ ion behaves as a hydrophobic site due to the three positively charged hydrogen atoms that hinder close approach from other hydrogen atoms towards the oxygen center.[3] Since the H_3O^+ ion and the H_2O molecule favor three and four hydrogen bonds, respectively, clusters are stabilized with a maximized number of hydrogen bonds by having the H_3O^+ ion on the surface and a water molecule inside the cage. Furthermore, in water clusters, an amphiphilic species such as a H_3O^+ ion favors the surface to maximize the polarization-driven binding energy, unless the cluster size is large.

Thus, using the empirical structure–energy relationship obtained from the energies of numerous structures based on the DFTB, B3LYP, MP2, and CPMD calculations, we find a simple and reasonable approach to locate the most-probable lowest-energy structures for these clusters: 1) the H_3O^+ ion tends to be on the surface, and favors a specific-site (S-site) hydrogen atom bonded by three ADD-type water molecules unless the surface has high curvature; 2) water molecules tend to favor four hydrogen bonds (AADD type) and three hydrogen bonds (AAD and ADD types) over two hydrogen bonds (AD, DD, and AA types) unless the increase in strain energy is larger than an additional hydrogen-bond energy gain, which sometimes occurs for an AADD-type hydrogen bond; 3) H_d atoms tend to be maximally distributed with least clustering to minimize the H–H repulsions; 4) the internal water molecule is favored to maximize up to four hydrogen bonds, and its orientation tends to have a strong charge–dipole interaction with the H_3O^+ ion; 5) contiguous long hydrogen-bond relays that have the same helicity as the OH orientations tend to stabilize the cluster with enhanced-polarized hydrogen bonds, and these cyclic hydrogen bonds generate nearly isoenergetic conformational isomers by changing the orientation of the OH helicity.[15]

The magic cluster $[H(H_2O)_{21}]^+$ has well-packed compact PD structures with nine AAD-type H_d atoms. Seven isoenergetic conformers (within < 0.3 kcal mol^{-1}) are formed with different cyclic OH orientations (Figure 1 a, b); the H_3O^+ ion is on the surface of the cage (21A structures). Based on B3LYP/aug-cc-pVDZ calculations, we found that the surface structure is 5–10 kcal mol^{-1} more stable than the internal structure (i.e., with the H_3O^+ ion inside the cage with ten H_d atoms) because of the presence of one additional hydrogen bond and the polarization effect.[17] In CPMD simulations,[18] when H_3O^+ is put inside a PD at 100 K, the proton is ejected out to the surface in about 1 ps, which is followed by rearrangement toward the S-site in 0.5 ps by the Grotthuss mechanism.

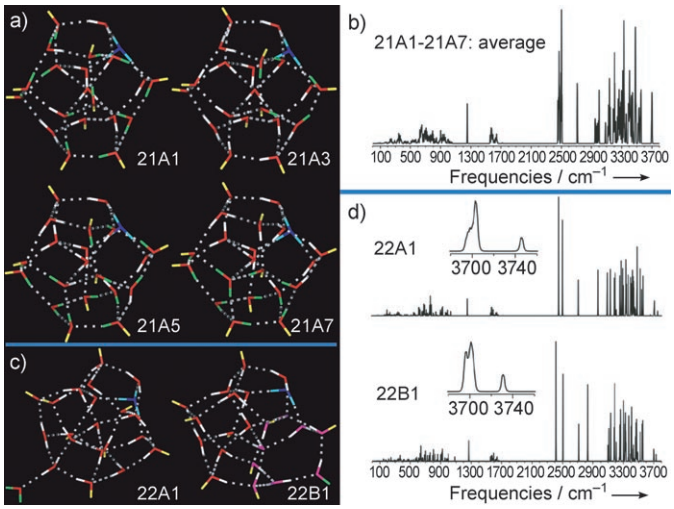

Figure 1. Most-stable conformers of $[H(H_2O)_{21}]^+$ and $[H(H_2O)_{22}]^+$. a) Seven nearly isoenergetic lowest-energy conformers of $[H(H_2O)_{21}]^+$ (only four of which are shown), which have nine ADD-type H_d atoms for the PD (5^{12}) topology with the least-clustered hydrogen bonds; 21A2,4,6 have the opposite helicities to those of 21A1,3,5, respectively; H_d atoms are yellow; cyclic helicity H atoms are green; protonated water molecules have blue O atoms and cyan H atoms. b) Averaged IR spectra of the seven isomers 21A1–21A7. c) Two nearly isoenergetic conformers, 22A1 and 22B1, of $[H(H_2O)_{22}]^+$, which have one A-type H_d (green) and one AD-type H_d (green); O atoms of the six-membered rings are magenta. d) IR spectra of 22A1 and 22B1. The molecular structures were drawn with the POSMOL program.[20]

Based on MP2/aug-cc-pVDZ calculations, we found that the most plausible realistic conformers of $[H(H_2O)_{20}]^+$ have structures with one water molecule being excluded from the surface of the PD structure of $[H(H_2O)_{21}]^+$. They show a strong AD peak, which is in agreement with other experiments.[4,5]

$[H(H_2O)_{22}]^+$ is predicted to have two nearly isoenergetic conformers with intriguing structures arising from one extra water molecule either sitting above or intruded into the PD structure of $[H(H_2O)_{21}]^+$ (Figure 1 c and d): 1) one water molecule (A type) on the top of the surface of the PD structure is singly hydrogen-bonded to one of AAD-type H_d atoms opposite the H_3O^+ ion (22A1); 2) a $5^{10}6^2$ topological structure has nine AAD- and one AD-type H_d atoms (22B1), with one water molecule inserted between two loosely hydrogen-bonded water molecules of the PD structure. These two structures clearly demonstrate why $[H(H_2O)_{21}]^+$ is particularly stable whereas $[H(H_2O)_{22}]^+$ is transient (or less stable) and explains their magic/antimagic natures. This difference in stability is also evidenced from the MP2/aug-cc-pVDZ binding energies with a B3LYP/aug-cc-pVDZ zero-point energy (ZPE) correction for $[H(H_2O)_{20}]^+$, $[H(H_2O)_{21}]^+$, and $[H(H_2O)_{22}]^+$, which are 12.26, 12.29, 12.11 kcal mol^{-1} per water molecule, respectively.

For $[H(H_2O)_{21}]^+$, all three levels of theory—DFTB, B3LYP/aug-cc-pVDZ, and MP2/aug-cc-pVTZ—give the lowest energy for the PD structure among the various structures that we have investigated. However, for $[H(H_2O)_{20}]^+$ and $[H(H_2O)_{22}]^+$, the three levels give different lowest-energy structures. Nevertheless, the potential surface on the local minimum does not vary significantly at the different levels of theory, and hence the three methods give similar frequencies for the same type of structure, which is predicted as a (local) minimum. Thus, for $[H(H_2O)_{20}]^+$ and $[H(H_2O)_{22}]^+$, the spectral study at the CPMD level is only reliable around the local region near the local minimum. However, for $[H(H_2O)_{21}]^+$ the PD structure is particularly stable, and thus the potential surface near the PD structure is reasonably well represented by most theoretical methods. Therefore, for $[H(H_2O)_{21}]^+$, we carried out first-principles CPMD simulations to analyze the thermal and dynamic effects. Nine sets of simulations were performed at 50 to 295 K for 6 ps each.

Figure 2 shows the O–O and O–H radial distribution functions (RDFs) for the last 4 ps sampled, some thermodynamic properties, and snapshots of the $[H(H_2O)_{21}]^+$ cluster at different temperatures. At 195 K, the structure is quite open and is starting to show glassy phenomena (Figure 2 c). The structure at 245 K has on average about 15 H_d atoms; however, it still retains the precluster characteristic of the PD topology. At 270 K the precluster moiety for the formation of the PD topology is completely lost, and the internal water molecule loses its four hydrogen bonds. Thus, the structure starts to have free water molecules, which results in evaporation as evidenced from a peak in the heat capacity (C_v) arising from a phase transition. It was possible to obtain the initial structures before the simulation of the cooling-down process of the CPMD configurations at 245 K (with 15 H_d atoms), but not from those at 270 K (with 18 H_d atoms and one/two freelike water molecules). The simulations also show that the protonated water molecule continues as an Eigen form below 100 K. The percentage of the Zundel form continuously increases with rising temperature, from about 1 % at 125 K to about 20 % at 270 K.

Figure 3 shows the power spectra of the simulations at various temperatures. The AAD- and ADD-type OH_d peaks (≈ 3700 and ≈ 3580 cm^{-1}) are in good agreement with the experimental spectra. As the number of AD-type H_d atoms increases with increasing temperature, the AD peak appears at 3715–3720 cm^{-1} above 170 K and is separated from the AAD peak by about 20 cm^{-1}. The ADD peak is not distinguishable at 50 and 100 K due to the presence of other

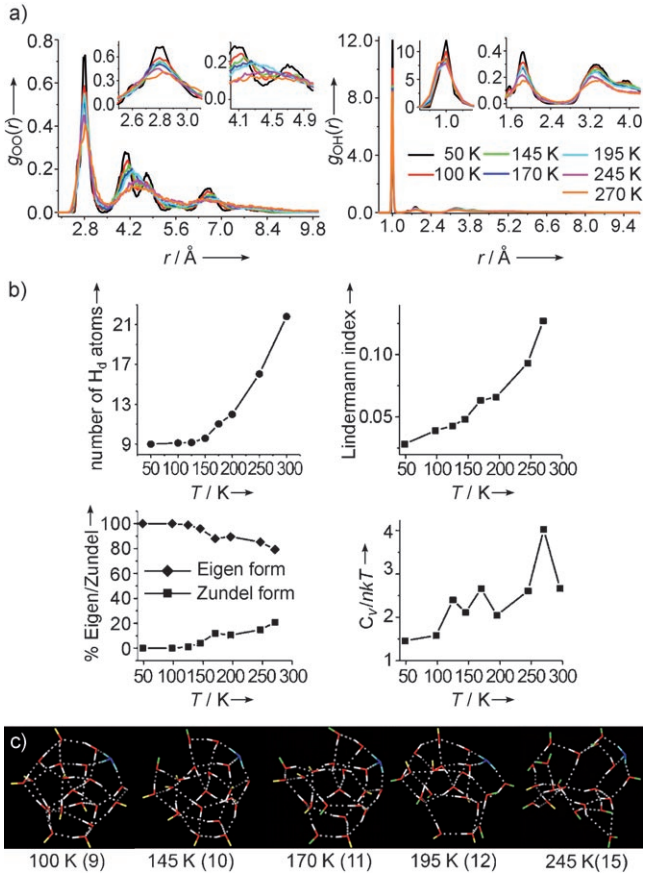

Figure 2. Structural and thermodynamic properties of $[H(H_2O)_{21}]^+$ at various temperatures: a) O–O and O–H RDFs. b) Average number of H_d atoms; Lindemann index; percentage of Eigen and Zundel forms; heat capacity; n = number of atoms. At 145 K, the second and third hydration shells in O–O (4.1, 4.7 Å) and O–H (3.3, 3.9 Å) RDFs start to merge, and from 170 K onwards the two peaks are not distinguishable. The average number of H_d atoms is strongly correlated with the Lindemann index, that is, the root-mean-square deviation of all the interatomic distances. c) Temperature-dependent representative structures (number of H_d atoms in parentheses). The instantaneous structure with ten H_d atoms at 145 K has two AD-type H_d atoms (AAD-type H_d atoms: yellow; AD-type H_d atoms: green).

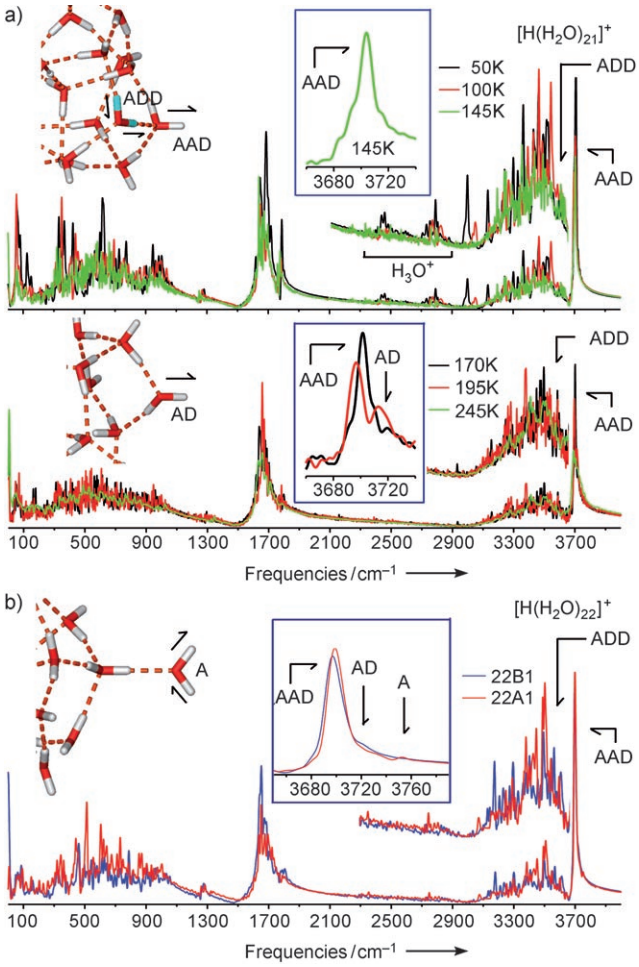

Figure 3. Power spectra of $[H(H_2O)_{21}]^+$ and $[H(H_2O)_{22}]^+$ (frequencies scaled by 1.049). a) $[H(H_2O)_{21}]^+$ at varying temperatures, insets show the expanded spectra to distinguish the AAD and AD peaks. The AAD- and ADD-type OH_d peaks appear at ≈3770 and ≈3580 cm^{-1}, respectively. As the temperature increases, the peaks broaden due to the structural fluctuation and deformation. Despite the presence of configurations with an extra AD-type H_d at 145 K, the AD peak does not appear because of the unusual dynamic effect associated with the flexible potential surface driven by proton mobility as the AD-type OH keeps changing its nature during simulations (towards ADD and AAD types). b) The two most-stable conformers (22A1, 22B1) of $[H(H_2O)_{22}]^+$ at 125 K. A small shoulder at 3724 cm^{-1} corresponds to AD-H_d atoms, and another small peak at 3755 cm^{-1} corresponds to A-H_d atoms, both of which show surprising dynamic effects.

strong peaks nearby, but becomes noticeable as other peaks weaken from 125 K onwards.

The most controversial issue of the spectra is that experiments do not find two key theoretical peaks that correspond to the H_3O^+ ion (≈2500 cm^{-1} and ≈2700 cm^{-1}). As the temperature increases, the peak at about 2500 cm^{-1} rapidly disappears before 100 K, while the peak at about 2750 cm^{-1} slowly diminishes and only this peak represents the unique Eigen feature at about 100 K. Even this peak becomes negligible at 125 K, and eventually disappears above 145 K. As the protonated water molecule on the surface is mostly in the Eigen form at 125 K, the dynamics due to minor fluctuations play a crucial role in defining the vibrational frequencies for the following reason: the energy barrier of a proton transfer from the H_3O^+ moiety in $[H(H_2O)_{21}]^+$ to the hydrogen-bonded oxygen atom in the adjacent water molecule is very low, which is reflected by the high proton mobility. This low barrier arises because each hydrogen atom of the H_3O^+ ion can be electronically shared by oxygen atoms of adjacent water molecules and from electrostatic and polarization effects. Above 125 K, the thermally induced large dynamic motion of the proton on the highly flattened anharmonic-potential-energy surface leads to the complete depletion of the peaks at about 2500 and 2700 cm^{-1}.[15]

The quantum effect for the proton motion is significant. However, the energy barrier of the DFT potential tends to be smaller than that of the more accurate ab initio results. Thus, the zero-point energy correction, which is the dominant quantum effect, is taken into account already (or over-compensated) due partly to the cancellation of errors. The

underestimated errors in the energy barriers ($> \approx 1$ kcal mol^{-1}) are greater than the small quantum effect (≈ 0.5 kcal mol^{-1} for $[H_9O_4]^+$).[2b] Consequently, the quantum effect is most likely to play a small role compared with the accuracy of the potential surface. Furthermore, the underestimation of the potential barriers in the DFT calculation happens to partially reflect the quantum-tunneling-driven effective barrier for the accurate ab initio potential surface. In this regard, we believe that the CPMD results realistically match the experimental observation. However, any small energy difference would need to be confirmed with more accurate calculations.

The heat capacity C_v (Figure 2b) shows a small peak at about 125 K due to the beginning of Zundel formation, but the IR peak at about 1000 cm^{-1}, which is the unique Zundel feature of the spectrum, cannot be measured. Nevertheless, the peak at around 1800 cm^{-1}, which corresponds to the HOH bending mode of both Eigen and Zundel forms (in contrast to the water-bending mode at ≈ 1700 cm^{-1}) is seen as a very weak proton signature below around 175 K.

Based on our predicted temperature-dependent spectra, we estimate the experimental temperature that produced the IR spectrum of $[H(H_2O)_{21}]^+$ reported by Shin et al. (no peaks for AD-type H_d atoms and H_3O^+, but a distinguishable peak for AAD-type H_d atoms) to be around 150 K,[5] whereas that reported by Miyazaki et al.[4] (a clear AD peak separated from the AAD peak by 20 cm^{-1}) we estimate was taken at around 175 K, which is in agreement with the authors' claim. We note that this latter prediction agrees with a recent experiment of Wu et al.[6]

For $[H(H_2O)_{22}]^+$, the A-type H_d peak (3746 cm^{-1}) in the IR spectra of 22A1 at 0 K and 50 K almost completely disappears in the power spectra at 125 K owing to large thermally induced dynamic motion. This motion is caused by strong anharmonic coupling (which arises from the flexible potential surface and involves the mobility of the hydrogen atom) between the antisymmetric and symmetric vibrational modes of this singly hydrogen-bonded A-type dangling water molecule (A-wat).[15] With increasing temperature, the A-wat outside the PD cage moves widely, and thus the donor hydrogen atom of the AADD-type water molecule that involves the hydrogen bond with the A-wat also moves significantly and affects the potential surface of the A-wat. In this situation, the two OH bonds of the A-wat (even though the bending angle is kept almost constant with only a small variation) can orient randomly through flapping and torsional rotation. Thus, the change in potential for the A-wat affected by the donor hydrogen atom and OH bond of the AADD-type water molecule involves anharmonic coupling of the two OH bonds of the A-wat. Consequently, an increase in temperature leads to a drastic increase in the anharmonic coupling effect,[19] which results in small broad peaks near the difference in value of the two OH frequencies. At higher temperatures, all these peaks disappear.

This unexpected dynamic behavior, which demonstrates the near-complete suppression of the OH peak, is different from the common dynamic effect. In the common dynamic effect, the isolated water monomer has a predefined rigid potential surface for which the corresponding IR peak is simply broadened. This peak reflects the average of the ensemble and does not diminish as each ensemble has a similar frequency and similar intensity. In the power spectra of 22B1 at 125 K, the strong AD-type peak (3724 cm^{-1}) also almost disappears. All previous work has focused in vain on finding structures without AD-type H_d for this antimagic cluster, whereas we find a surprising dynamic effect: that either an A-type or AD-type H_d does exist but the peak is highly suppressed. This finding goes against conventional wisdom and is extremely important as OH peaks of IR spectra have been extensively exploited for the structural identification of diverse hydrogen-bonded clusters.

The present analysis provides answers to previously unresolved problems of magic and antimagic protonated water clusters and accounts for the difference in structure of clusters that have the H_3O^+ ion on the surface compared with those clusters that have internal ions such as Cs^+, K^+, and NH_4^+. Thus, very accurate ab initio calculations are able to predict the right structures. The dynamic effect on the stretching peak of the hydrogen bond would resolve many other problems in this area of cluster chemistry and allow analysis of spectroscopic fingerprints.

Received: November 22, 2005
Revised: February 25, 2006
Published online: May 3, 2006

Keywords: cluster compounds · density functional calculations · molecular dynamics · vibrational spectroscopy · water chemistry

[1] a) J. M. Headrick, E. G. Diken, R. S. Walters, N. I. Hammer, R. A. Christie, J. Cui, E. M. Myshakin, M. A. Duncan, M. A. Johnson, K. D. Jordan, *Science* **2005**, *308*, 1765 – 1769; b) K. R. Asmis, N. L. Pivonka, G. Santambrogio, M. Brümmer, C. Kaposta, D. M. Neumark, L. Wöste, *Science* **2003**, *299*, 1375 – 1377.
[2] a) D. Wei, D. R. Salahub, *J. Chem. Phys.* **1997**, *106*, 6086 – 6094; b) D. Mark, M. Tuckermann, E. J. Hutter, M. Parrinello, *Nature* **1999**, *397*, 601 – 604.
[3] H. M. Lee, P. Tarakeshwar, J. W. Park, M. R. Kolaski, Y. J. Yoon, H.-B. Yi, W. Y. Kim, K. S. Kim, *J. Phys. Chem. A* **2004**, *108*, 2949 – 2958.
[4] M. Miyazaki, A. Fujii, T. Ebata, N. Mikami, *Science* **2004**, *304*, 1134 – 1137.
[5] J.-W. Shin, N. I. Hammer, E. G. Diken, M. A. Johnson, R. S. Walters, T. D. Jaeger, M. A. Duncan, R. A. Christie, K. D. Jordan, *Science* **2004**, *304*, 1137 – 1140.
[6] C.-C. Wu, C.-K. Lin, H.-C. Chang, J.-C. Jiang, J.-L. Kuo, M. L. Klein, *J. Chem. Phys.* **2005**, *122*, 07431519.
[7] a) J. Q. Searcy, J. B. Fenn, *J. Chem. Phys.* **1974**, *61*, 5282 – 5288; b) X. Yang, A. W. Castleman, Jr., *J. Am. Chem. Soc.* **1989**, *111*, 6845 – 6846; c) T. F. Magnera, D. E. David, J. Michl, *Chem. Phys. Lett.* **1991**, *182*, 363 – 370.
[8] a) L. Ojamae, I. Shavitt, S. J. Singer, *J. Chem. Phys.* **1998**, *109*, 5547 – 5564; b) S. S. Iyengak, T. J. F. Day, G. A. Voth, *Int. J. Mass Spectrom.* **2005**, *241*, 197 – 204; c) A. Khan, *Chem. Phys. Lett.* **2000**, *319*, 440 – 450; J.-L. Kuo, M. L. Klein, *J. Chem. Phys.* **2005**, *122*, 02451619.
[9] a) M. P. Hodges, D. J. Wales, *Chem. Phys. Lett.* **2000**, *324*, 279 – 288; b) T. James, D. J. Wales, *J. Chem. Phys.* **2005**, *122*, 134306.
[10] E. D. Sloan, Jr., *Nature* **2003**, *426*, 353 – 359.
[11] T. S. Zwier, *Science* **2004**, *304*, 1119 – 1120.

[12] a) J. Kim, K. S. Kim, *J. Chem. Phys.* **1998**, *109*, 5886 – 5895; b) H. M. Lee, S. B. Suh, J. Y. Lee, P. Tarakeshwar, K. S. Kim, *J. Chem. Phys.* **2000**, *112*, 9759 – 9772; c) K. S. Kim, P. Tarakeshwar, J. Y. Lee, *Chem. Rev.* **2000**, *100*, 4145 – 4186. d) S. Lee, J. Kim, S. J. Lee, K. S. Kim, *Phys. Rev. Lett.* **1997**, *79*, 2038 – 2041; e) H. M. Lee, S. B. Suh, P. Tarakeshwar, K. S. Kim, *J. Chem. Phys.* **2005**, *122*, 044309.

[13] T. Frauenheim, G. Seifert, M. Elstner, T. Niehaus, C. Köhler, M. Amkreutz, M. Sternberg, Z. Hajnal, A. D. Carlo, S. Suhai, *J. Phys. Condens. Matter* **2002**, *14*, 3049 – 3084.

[14] a) K. S. Kim, M. Dupuis, G. C. Lie, E. Clementi, *Chem. Phys. Lett.* **1986**, *131*, 451 – 456; b) K. S. Kim, *Bull. Korean Chem. Soc.* **1993**, *14*, 18 – 20.

[15] Refer to Supporting Information.

[16] F. Sobott, A. Wattenberg, H.-D. Barth, B. Brutschy, *Int. J. Mass Spectrom.* **1999**, *185–187*, 271 – 279.

[17] Gaussian 03 (Revision A.1), M. J. Frisch, G. W. Trucks, H. B. Schlegel, G. E. Scuseria, M. A. Robb, J. R. Cheeseman, J. A. Montgomery, Jr., T. Vreven, K. N. Kudin, J. C. Burant, J. M. Millam, S. S. Iyengar, J. Tomasi, V. Barone, B. Mennucci, M. Cossi, G. Scalmani, N. Rega, G. A. Petersson, H. Nakatsuji, M. Hada, M. Ehara, K. Toyota, R. Fukuda, J. Hasegawa, M. Ishida, T. Nakajima, Y. Honda, O. Kitao, H. Nakai, M. Klene, X. Li, J. E. Knox, H. P. Hratchian, J. B. Cross, C. Adamo, J. Jaramillo, R. Gomperts, R. E. Stratmann, O. Yazyev, A. J. Austin, R. Cammi, C. Pomelli, J. W. Ochterski, P. Y. Ayala, K. Morokuma, G. A. Voth, P. Salvador, J. J. Dannenberg, V. G. Zakrzewski, S. Dapprich, A. D. Daniels, M. C. Strain, O. Farkas, D. K. Malick, A. D. Rabuck, K. Raghavachari, J. B. Foresman, J. V. Ortiz, Q. Cui, A. G. Baboul, S. Clifford, J. Cioslowski, B. B. Stefanov, G. Liu, A. Liashenko, P. Piskorz, I. Komaromi, R. L. Martin, D. J. Fox, T. Keith, M. A. Al-Laham, C. Y. Peng, A. Nanayakkara, M. Challacombe, P. M. W. Gill, B. Johnson, W. Chen, M. W. Wong, C. Gonzalez, J. A. Pople, Gaussian, Inc., Pittsburgh, PA, **2003**.

[18] Troulller–Martins pseudopotential; BLYP functionals with gradient correction; the energy cutoff value was 90 Ry; time step: 0.1 fs; CPMD code Version 3.7.2, CPMD, Copyright IBM Corp 1990 – 2001, Copyright MPI für Festkörperforschung Stuttgart 1997 – 2001.

[19] L. D. Landau, E. M. Lifshitz, *Mechanics*, Pergamon, 2nd ed., **1969**, pp. 84 – 87.

[20] S. J. Lee, H. Y. Chung, K. S. Kim, *Bull. Korean Chem. Soc.* **2004**, *25*, 1061 – 1064.

